

Supporting Material for:

A General Approach for Generating Fluorescent Probes to Visualize Piconewton Forces at the Cell Surface

Yuan Chang, Zheng Liu, Yun Zhang, Kornelia Galior, Jeffery Yang and Khalid Salaita*

Department of Chemistry, Emory University, Atlanta, GA, USA

This file includes:

Supplementary Figures

- Figure S1.** Synthesis, purification and characterization of the alkyne-TAMRA-PEG₂₄-cysteine conjugate
- Figure S2.** Synthesis of the cRGDfK thioester ligand
- Figure S3.** Synthesis, purification and characterization of ligand peptides cRGDfK, SHAVSS, PHSRN, HAVDING, GRGDS and PHSRN(SG)₄RGDS
- Figure S4.** Synthesis, purification, and characterization of a library of MTFM probes
- Figure S5.** Synthesis of zwitterion silane SBS
- Figure S6.** Preparation of the covalent azide-functionalized glass surfaces
- Figure S7.** Quenching efficiency by photobleaching TAMRA
- Figure S8.** Tension probe surface density
- Figure S9.** Synthesis, purification and characterization of the tandem biotin probe for measuring PEG extension as a function of passivation
- Figure S10.** Colocalization between tension signal and β 3-integrin-GFP
- Figure S11.** Tension signal dissipates following PFA fixation
- Figure S12.** Tension signal is dynamic, reversible, and actin dependent
- Figure S13.** Dynamic range of PEG₄₈ and PEG₂₄ tension probes
- Figure S14.** SHAVSS tension response is actin dependent and likely E-cadherin specific.
- Figure S15.** Fluorescence intensity change of MTFM probes over 64 hours

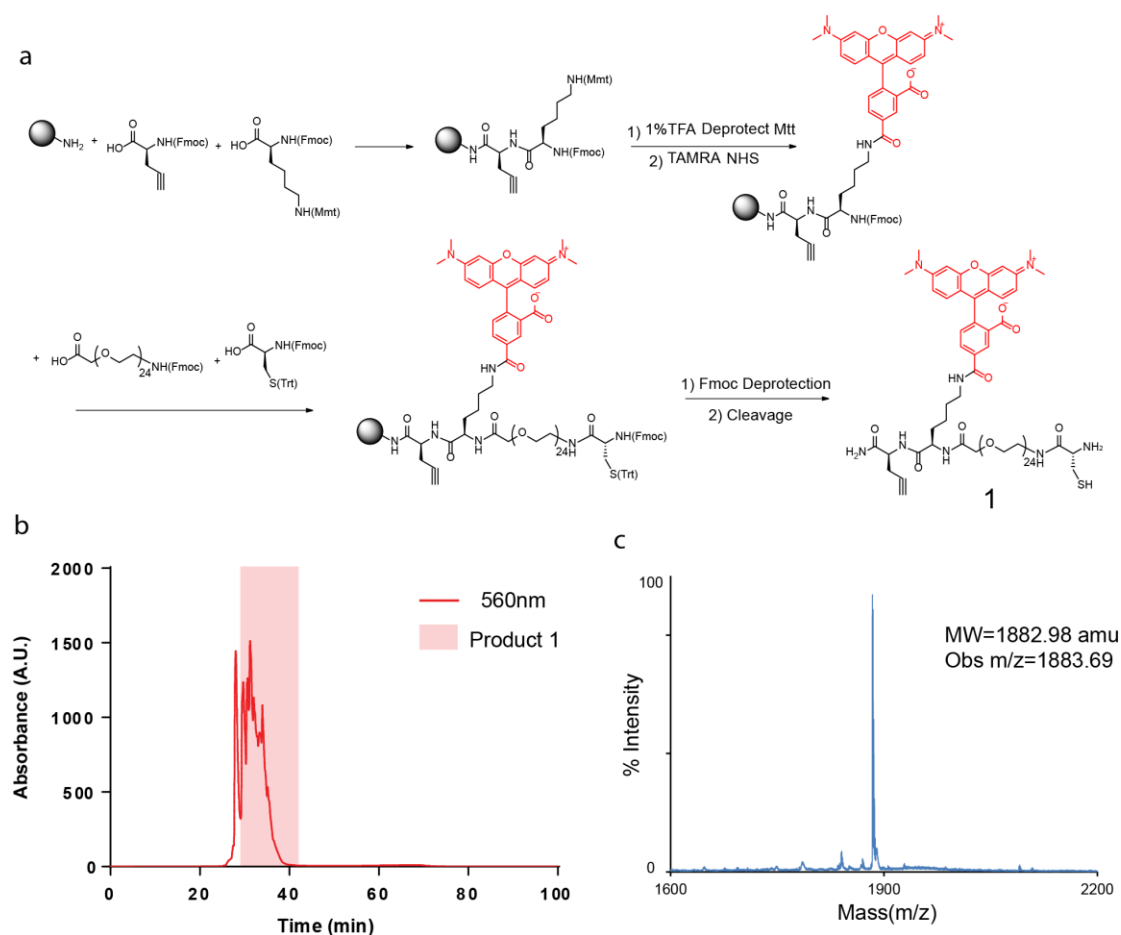
Materials and Methods

Supplementary Notes

1. Determination of the Förster distance of Alexa 488-TAMRA FRET pair and TAMRA-QSY9 FRET pair
2. Measuring the quenching efficiency (QE) of Alexa 488-TAMRA FRET pair and QSY9 and TAMRA-QSY9 FRET pair
3. Stepwise image analysis of cell tension using FRET and WLC models.

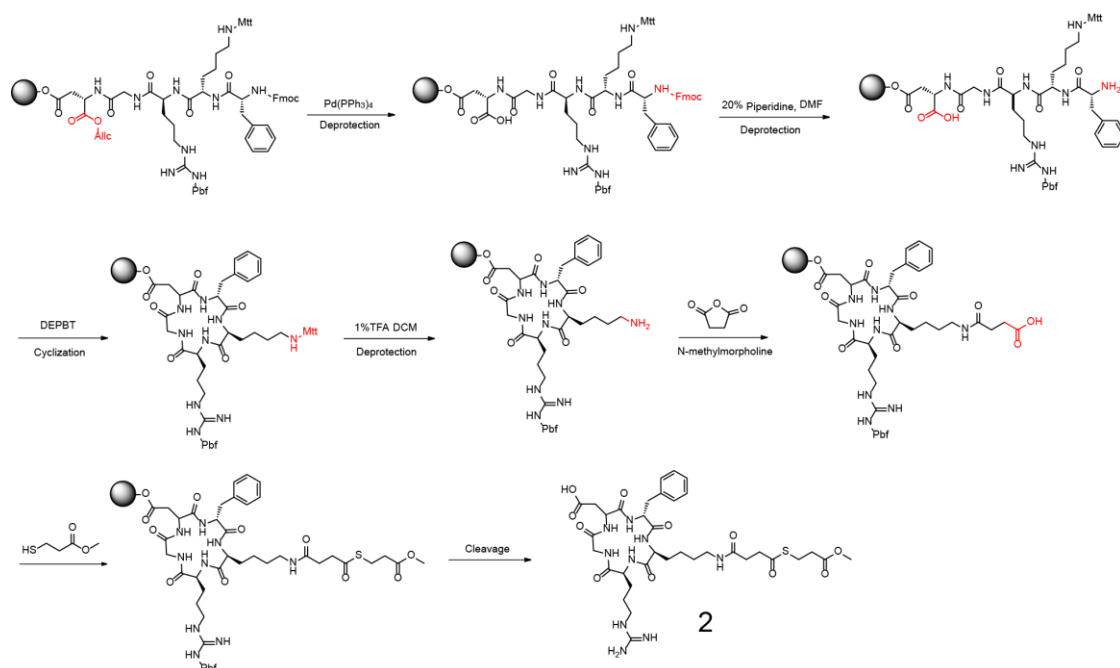
References

Supplementary figure S1. Synthesis, purification and characterization of the alkyne-TAMRA-PEG₂₄-cysteine conjugate



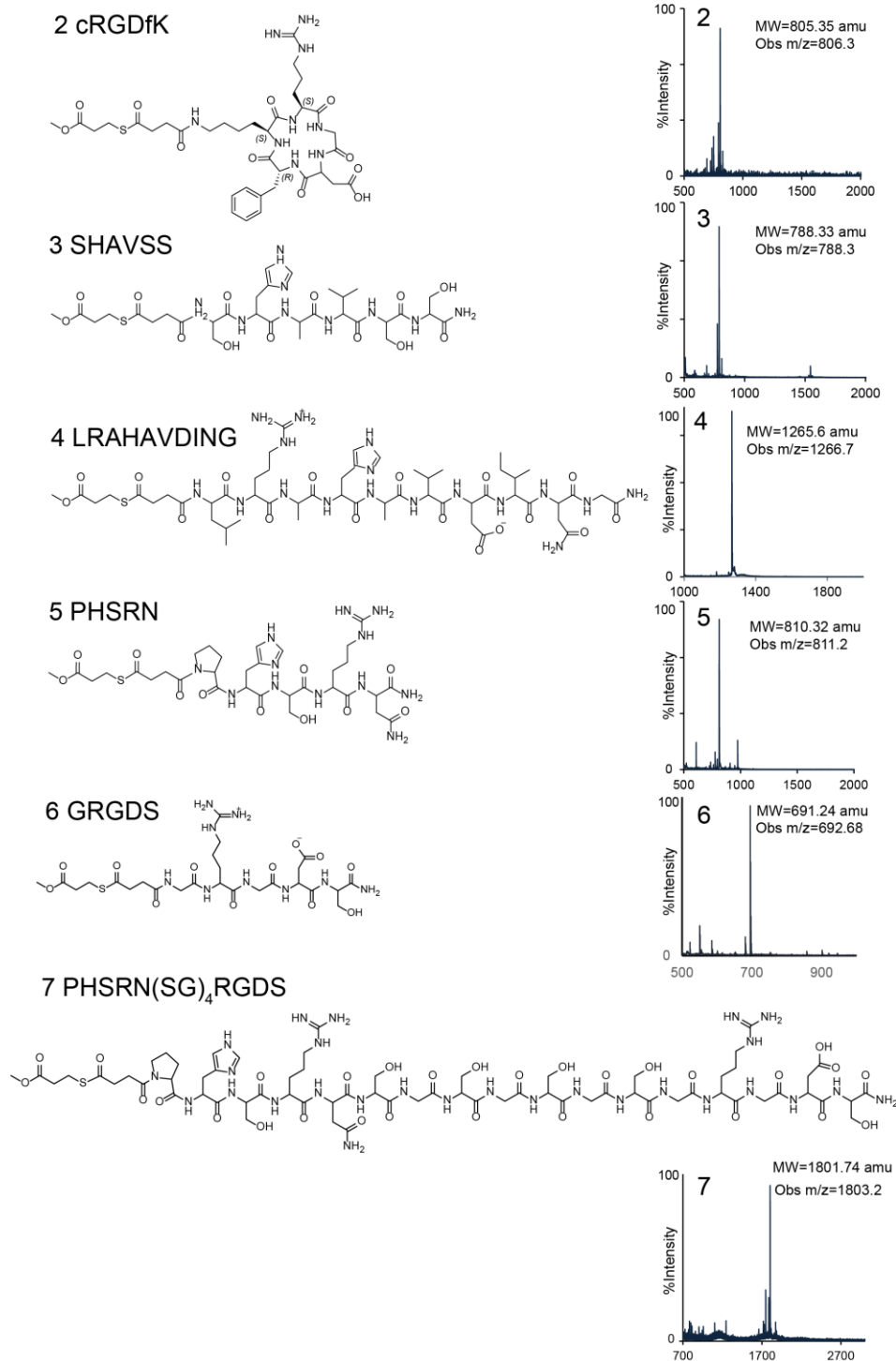
a) The tension probe was manually synthesized on a solid support and on-resin labeling was used to introduce the TAMRA dye. Specifically, Fmoc-L-propargylglycine, Fmoc-Lys(Mtt)-OH, Fmoc-PEG₂₄-OH were coupled sequentially following the standard Fmoc peptide synthesis procedures in a syringe. The Mtt protecting group of the lysine was selectively deprotected with 1% trifluoroacetic acid (TFA) in CH₂Cl₂. Subsequently, the resin was then treated with excess TAMRA succinimidyl ester in DMF. After deprotecting the Fmoc-PEG₂₄-OH with 20% piperidine in DMF, the Fmoc-Cys(Trt)-OH residue was coupled to the N-terminus of the peptide. After final Fmoc deprotection, the sensor was cleaved from resin with 95% TFA with triisopropylsilane (TIS) as a scavenger. The synthesized construct was purified and characterized by a diode array detector-equipped HPLC and MALDI-TOF MS. b) Reverse phase HPLC chromatogram of compound **1**. The absorbance was measured at 560 nm. 1 ml fractions were collected as they eluted off the column (flow rate = 1 ml/min from 8% to 100% Acetonitrile/water). c) The peaks were characterized by MALDI-TOF MS and the final SPPS product **1** (MW_{obs} = 1883.69; MW_{expected}=1882.98) was found to elute at 28-40 min. The yield of the product was >50%

Supplementary figure S2. Synthesis of the cyclic-RGDfK thioester



The synthesis of the cyclic-RGDfK thioester peptide was adapted from the protocol previously published by Xiao et al.¹ Briefly, Asp(OAll), Gly, Arg(pbf), Lys(mtt) and D-Phe were coupled on a CEM Liberty Microwave Synthesizer (Matthews, NC) using standard solid-phase peptide synthesis procedures using Fmoc chemistry and Rink Amide resins. After synthesis of the protected linear peptide, the resins were transferred into a syringe. The C-terminal allyl ester protecting group was then removed by treatment with $\text{Pd(PPh}_3)_4$ in $\text{CHCl}_3/\text{AcOH}/\text{N-methylmorpholine}$ 37:2:1 for 3h under a nitrogen atmosphere. The resin was washed carefully with DIPEA (5%) in DMF, and then the N-terminal Fmoc protecting group was removed by treatment with 20% piperidine in DMF. 5 equivalents of DEPBT and 2 equivalents of DIEA were then used to cyclize the peptide on resin. The cyclization reaction was carried out for 18 hours in DMF. Then, the Mtt protecting group of the lysine was selectively deprotected with 1% trifluoroacetic acid (TFA) in CH_2Cl_2 . The lysine amine was subsequently acylated with succinic anhydride. Thioester formation was accomplished on-resin by addition of methyl 3-mercaptopropionate, 4-dimethylaminopyridine (DMAP), and N-hydroxybenzotriazole (HOBt) using N,N'-diisopropylcarbodiimide (DIC) as a coupling reagent. Cleavage from the resin and removal of the remaining protecting groups were accomplished using TFA with triisopropylsilane (TIS) as a scavenger. The resulting peptide thioester, **2**, was precipitated from diethyl ether and purified by reversed phase HPLC. 1 ml fractions were collected as they eluted off the column (flow rate = 1 ml/min from 8% to 100% Acetonitrile/water). The yield of the product was >70%. The peptide was then characterized by HPLC and MALDI-TOF MS.

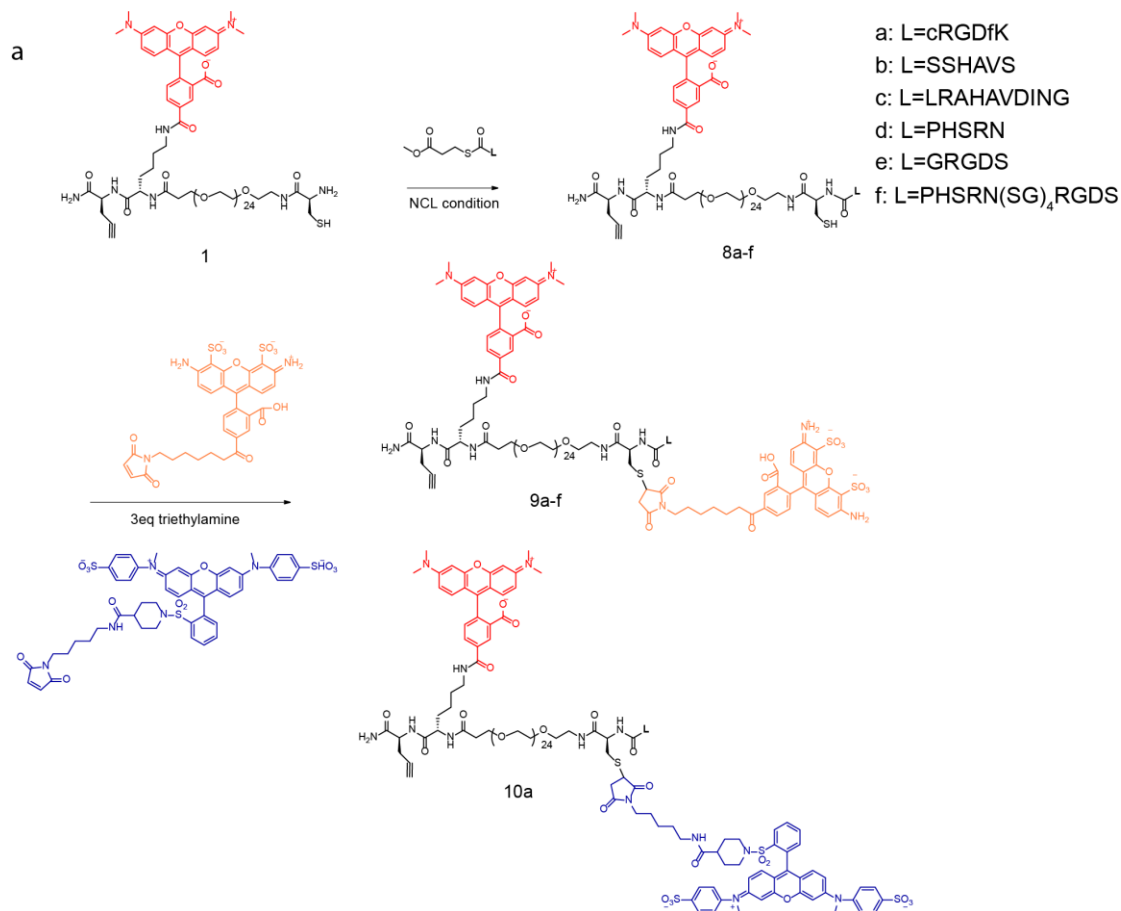
Supplementary figure S3. Synthesis, purification and characterization of a library of peptide thioesters



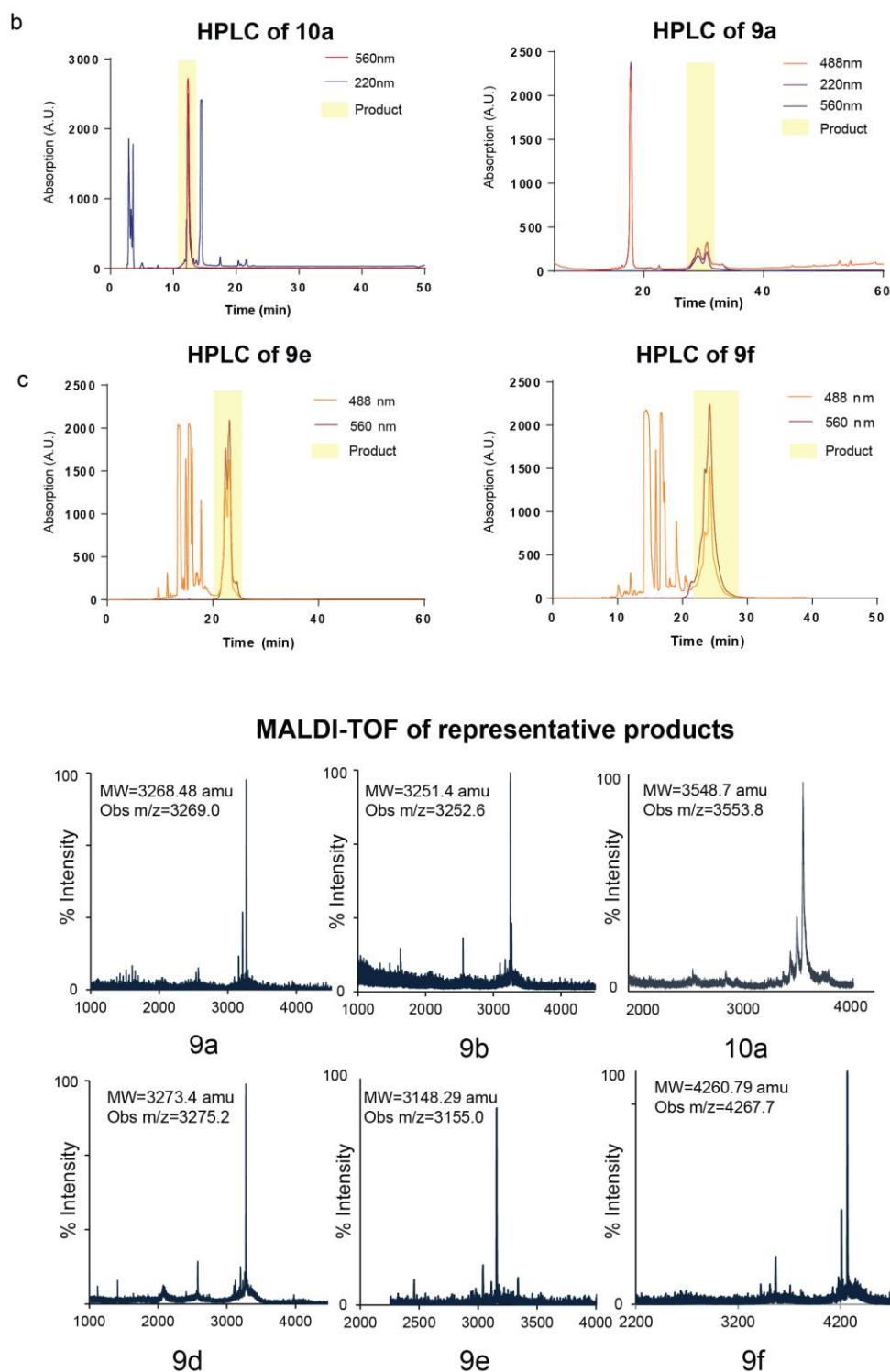
Standard solid-phase peptide synthesis was used to generate the peptides **3**, **4**, **5**, **6**, **7** on a CEM Liberty Microwave Synthesizer (Matthews, NC) following the protocol described in SI Figure S2. These peptides are then purified by reversed phase HPLC and characterized by HPLC and MALDI-TOF MS. 1 ml fractions were collected as they eluted off the column (flow rate = 1 ml/min from 8% to 100% Acetonitrile/water). The yield of the products was ranged from 60%-75%.

Supplementary figure S4. Synthesis, purification, and characterization of a library of MTFM probes

probes

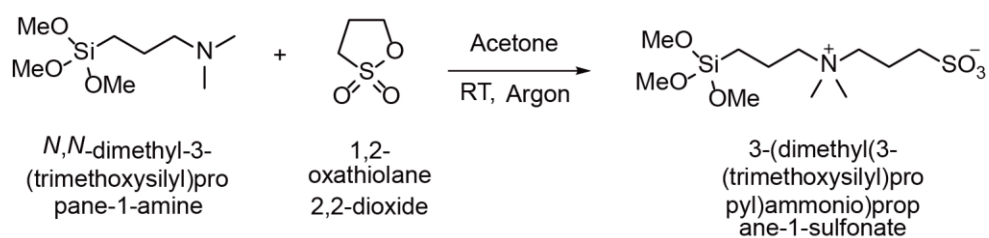


a) The native chemical ligation (NCL) reaction was used to conjugate peptide α -thioesters (**2-5**) to the tension probe, **1**. The NCL reaction was carried out by mixing **1** (10 mM) with 5 mM peptide thioester (**2-7**) in 20 mM sodium phosphate buffer (pH 7.5) containing 5 mM betaine and 30 mM sodium 2-mercaptoethanesulfonic acid (MPAA).² The reaction mixture was incubated for 24 hrs at room temperature. The thiol resulting from the NCL reaction in **8a-d** was subsequently coupled to a second dye/quencher via Michael addition. The reaction was carried out by mixing product **8a-d** with Alexa 488 maleimide or QSY 9 maleimide (**9a-f** and **10a**).



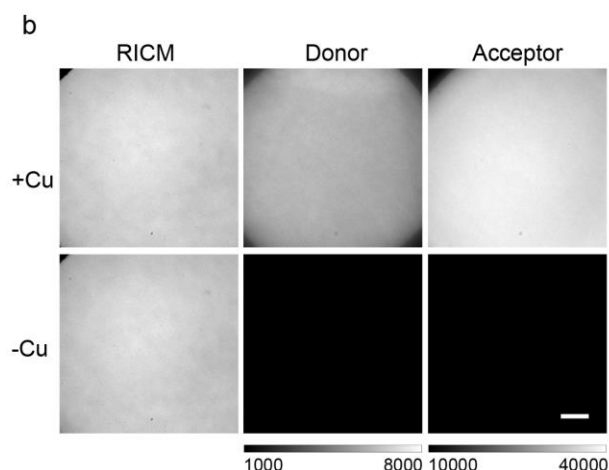
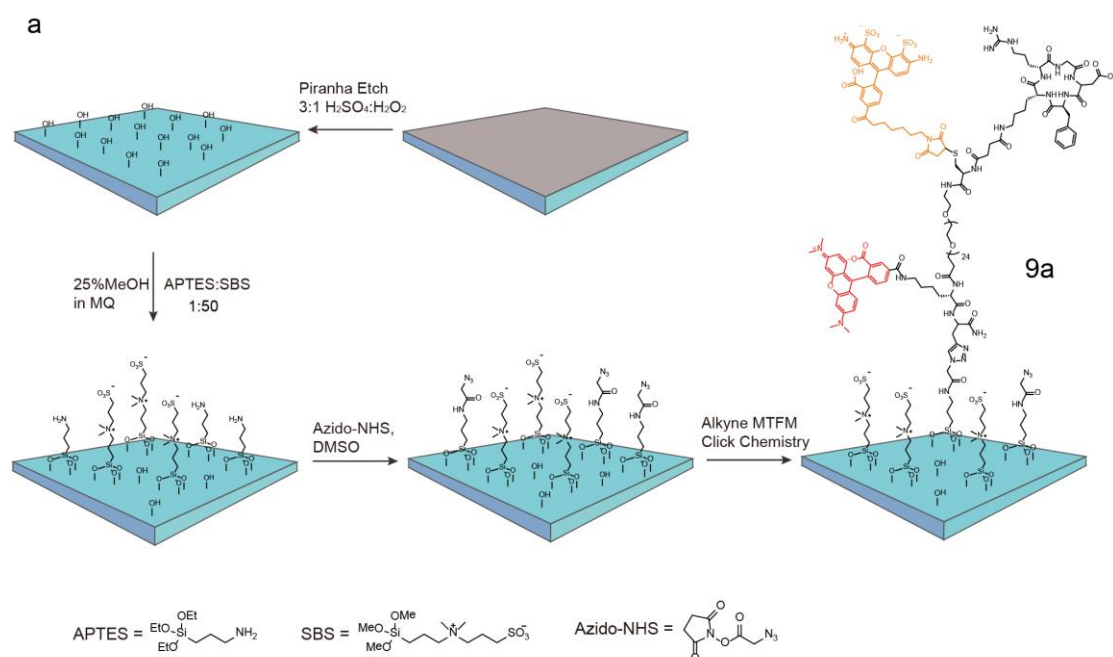
b) The final product was purified by HPLC and analyzed by MALDI-TOF MS. Reverse phase HPLC chromatogram of compound **9a**, **9e**, **9f** and **10a** are shown in SI Figure S4 b. The absorbance was measured at 220nm, 488nm and 560 nm. 1 ml fractions were collected as they eluted off the column (flow rate = 1 ml/min from 8% to 100%). The product of NCL reaction **8a** was found to elute at 12-13 min, and the final cRGDFK MTFM probe **9a** was found to elute at 28-32 min. c) The peaks were characterized by MALDI-TOF MS. The yields of all the products are greater than 95% according to integration of the area under the peaks from the HPLC chromatograms.

Supplementary figure S5. Synthesis of zwitterion silane SBS



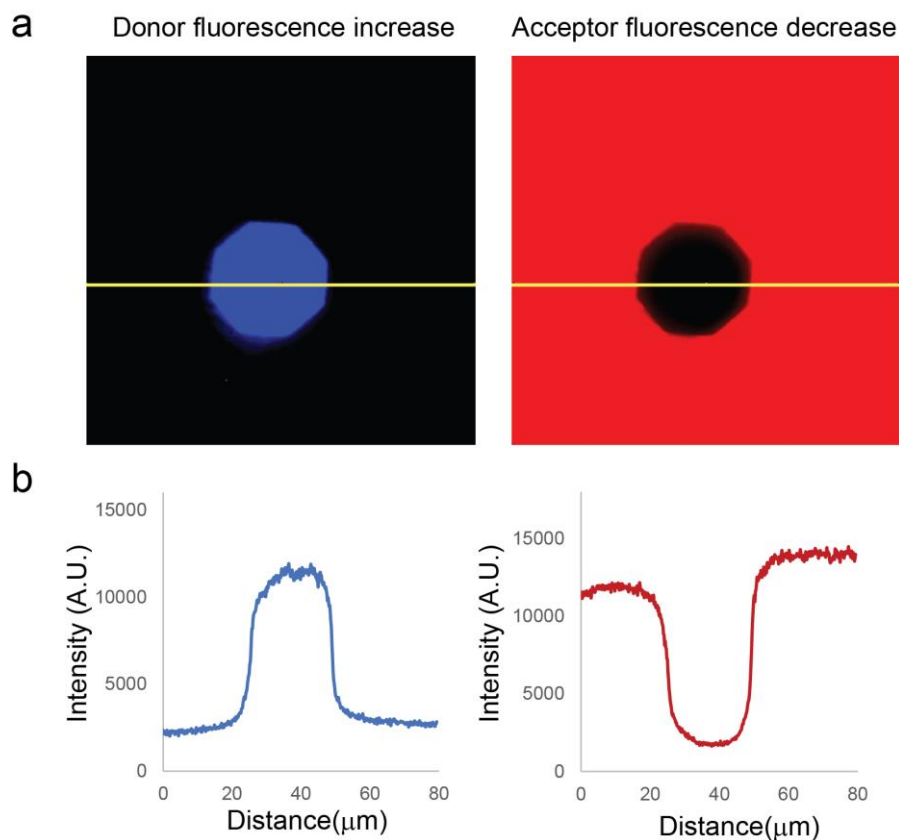
The synthesis of zwitterion siloxane (sulfo betaine silane, SBS), was adapted from Estephan et al³. 7.5 g of (N,N dimethyl- 3-aminopropyl) trimethoxysilane was added to 4.45 g of propane sultone in 37 mL of acetone under N₂. The reaction was stirred vigorously for 6 hr. The white precipitate was collected by vacuum filtration and washed twice with acetone. The white solid was then dried and stored under Ar. The yield was > 90%. Solution ¹H 300 MHz DMSO-6D and ¹³C CP/MAS solid state peak assignments and chemical shifts for the SBS are shown below. ¹H NMR (DMSO-6D, 300 MHz): δ 0.4-0.6 (B, t, 2H), 1.6-1.8 (C, m, 2H), 1.9-2.0 (G, m, 2H), 2.4-2.5 (D, t, 2H), 3.0 (E, s, 6H), 3.1-3.3 (F, m, 2H), 3.3-3.4 (H, m, 2H), 3.5 (A, s, 9H). ¹³C NMR (MAS 15 KHz, 125.8 MHz): δ 49 (A), 13.8 (B), 2.78 (C), 59.25 (D, F), 58 (E), 16.55 (F), 46 (G).

Supplementary figure S6. Preparation of the covalent azide-functionalized glass surfaces



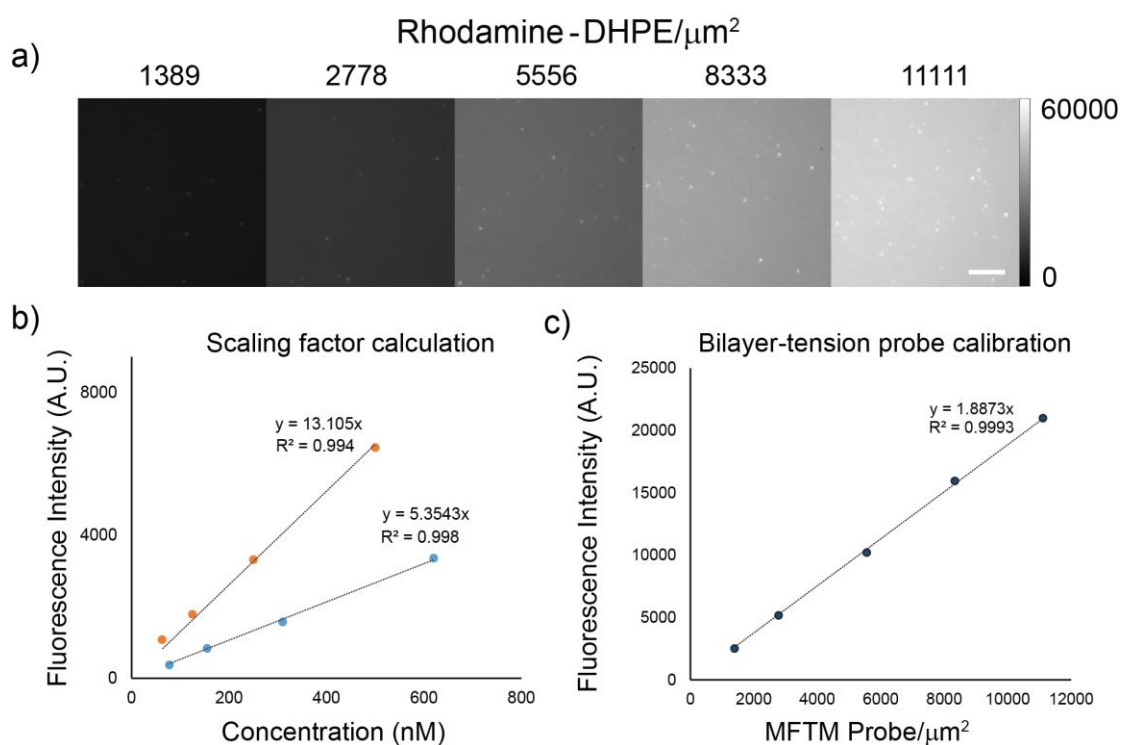
a) Glass coverslips (as described in Materials and Methods) were piranha-etched in order to produce a clean glass surface containing free terminal hydroxyl groups. A binary mixture of APTES and SBS at a molar ratio of 1: 50 was coupled to the hydroxyl surface groups of the glass coverslip to generate a surface presenting reactive amine and passivating zwitterion. The samples were then washed with methanol and water and dried under a stream of N_2 . Subsequently, azide N-hydroxysuccinimide ester dissolved in DMSO (5 mM) was coupled to the free amines on the coverslip to generating an azide functionalized surface. Finally, the tension probes (Alexa 488-TAMRA/PEG₂₄) were then covalently linked to the surface using copper-catalyzed Azide-Alkyne Huisgen cycloaddition. This was achieved by using a 50 μL solution containing 0.1-5 μM alkyne-terminated tension probe, 5 mM Cu-TBTA, and 10 mM ascorbic acid in 1:1 DMSO:H₂O. The reaction was allowed to proceed between two azide-functionalized coverslips for 5 min. b) A solution with no Cu-TBTA was used to generate control samples, showing that the tension probe primarily bound the surface through the Cu-catalyzed click reaction. (Scale bar 10 μm)

Supplementary figure S7. Quenching efficiency by photobleaching TAMRA



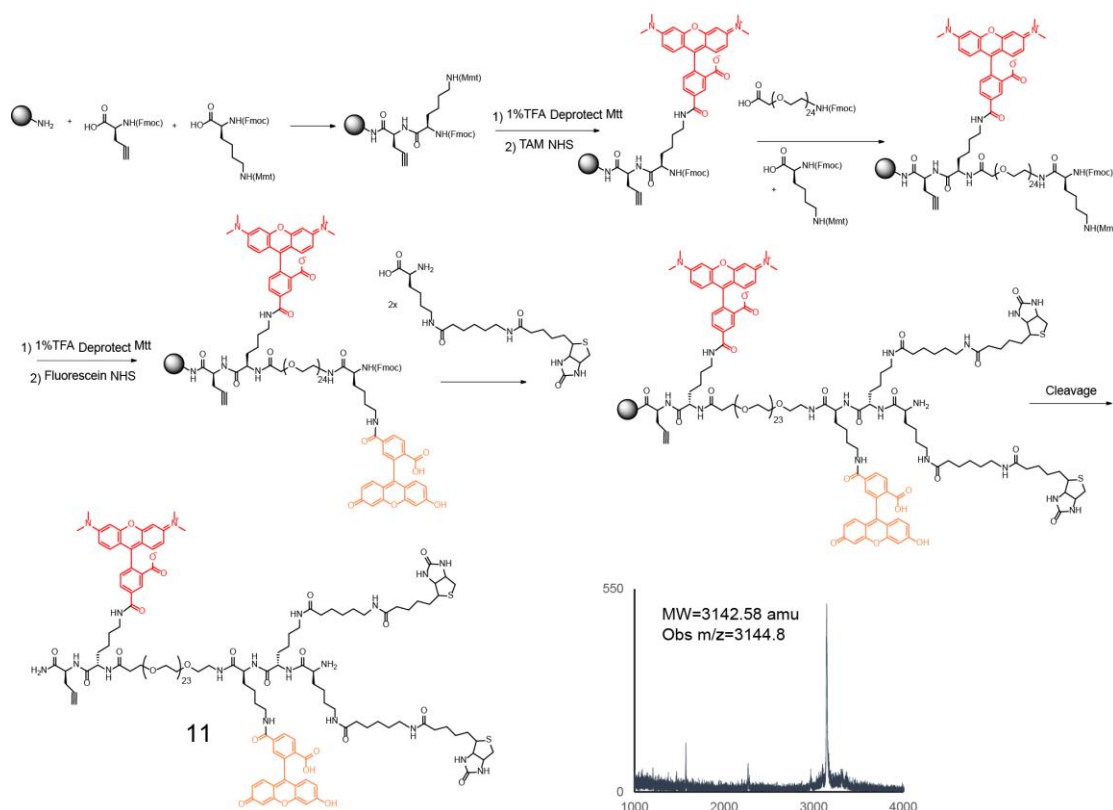
To verify the quenching efficiency of the TAMRA-Alexa488/PEG₂₄ tension probe, glass coverslips (as described in Materials and Methods) were passivated with SBS and modified with MTFM sensor **9a**. a) A focused 561 nm laser was used to photobleach the TAMRA acceptor for a 5 min duration (center area in a). Representative images of the donor and acceptor channels is shown in the top panel. b) Line scan analysis of the images showed that the Alexa 488 donor increased in brightness by 83% (left), while the TAMRA acceptor intensity decreased by 85% (right). This result indicated that the quenching efficiency of the TAMRA-Alexa488 pair is at least 83%.

Supplementary figure S8. Tension probe surface density



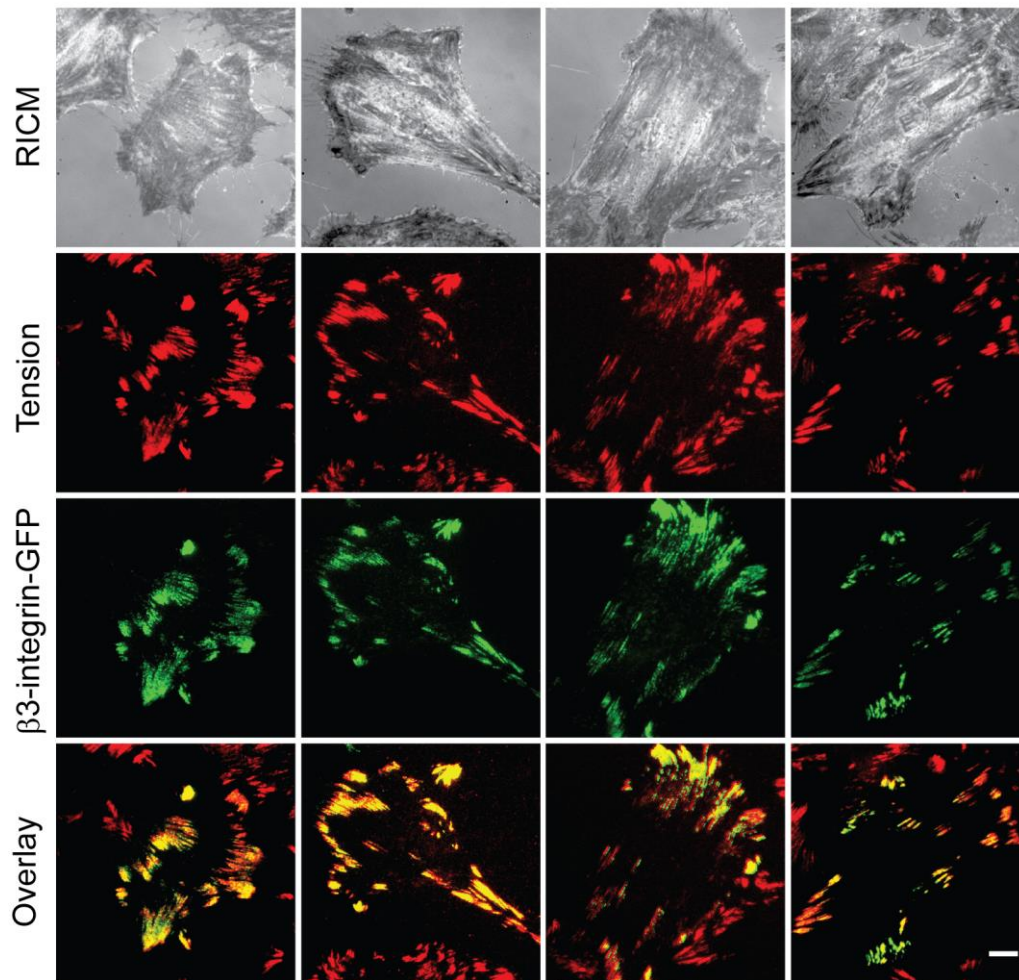
The surface density of the MTFM probes was determined using quantitative fluorescence microscopy with supported lipid bilayer standards.⁴ Supported bilayers for calibration standards containing rhodamine-DHPE mixed with DOPC were formed in glass-bottom 96 well plates. a) Fluorescence images showed calibration bilayers with increasing amounts of rhodamine-DHPE (scale bar = $10\mu\text{m}$). The fluorescence intensity of bilayers increases with increasing doping concentration (density) of rhodamine-DHPE. Each image corresponds to a single data point. b) In order to calibrate the fluorescence intensity of the tension probe against the lipid-conjugated rhodamine DHPE, we determined a scaling factor, F . To achieve this, the microscope was defocused into a solution of known lipid vesicle or tension probe, and the fluorescence intensity of the solution was recorded. The dotted lines represent linear regression fits, resulting in a scaling factor $F = \frac{k_{probe}}{k_{lipid}} = 2.44$. c) The calibrated tension probe surface density and fluorescence intensity were then plotted. The dotted line represents a linear regression fit of the five tension probe densities ($R^2 = 0.9993$).

Supplementary figure S9. Synthesis, purification, and characterization of the tandem biotin probe for measuring PEG extension as a function of passivation



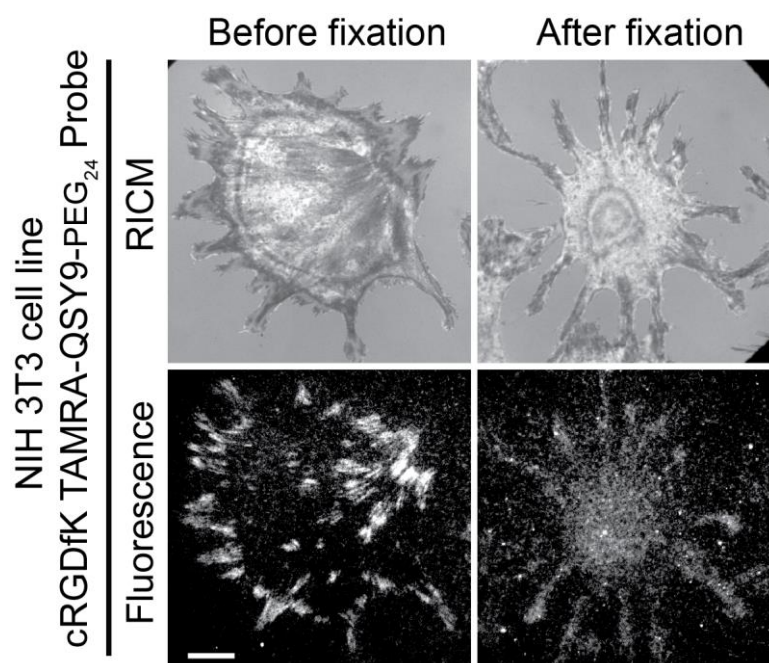
The tandem biotin probe was synthesized using manual SPPS and on-resin dye labeling in concordance with a procedure similar to that used for compound **1**. Briefly, Fmoc-L-propargylglycine, Fmoc-Lys(Mtt)-OH, were coupled sequentially following standard Fmoc peptide synthesis procedures in a syringe. The Mtt protecting group of the lysine was selectively deprotected with 1% TFA in CH₂Cl₂. The resin was then treated with excess TAMRA succinimidyl ester in DMF. After deprotecting the Fmoc on the terminal Lys residue, Fmoc-PEG₂₄-OH and Fmoc-Lys(Mtt)-OH residues were coupled to the peptide. The Mtt protecting group on the terminal Lys residue was then deprotected and treated with excess fluorescein succinimidyl ester with 5 molar excess of DIEA. Following this step, two Fmoc Lys(LC-LC-biotin)-OH residues were coupled to the peptide chain N-terminus. The tandem biotin probe was then cleaved from resin with 95% TFA, using triisopropylsilane (TIS) as a scavenger. 1 ml fractions were collected as they eluted off the column (flow rate = 1 ml/min from 8% to 100% Acetonitrile/water). The synthesized construct, **11**, was characterized by HPLC and MALDI-TOF MS. The yield of the products was >40%.

Supplementary figure S10. Colocalization between tension signal and β 3-integrin-GFP
NIH 3T3 Cells on cRGDfK TAMRA-QSY9-PEG₂₄ Sensor



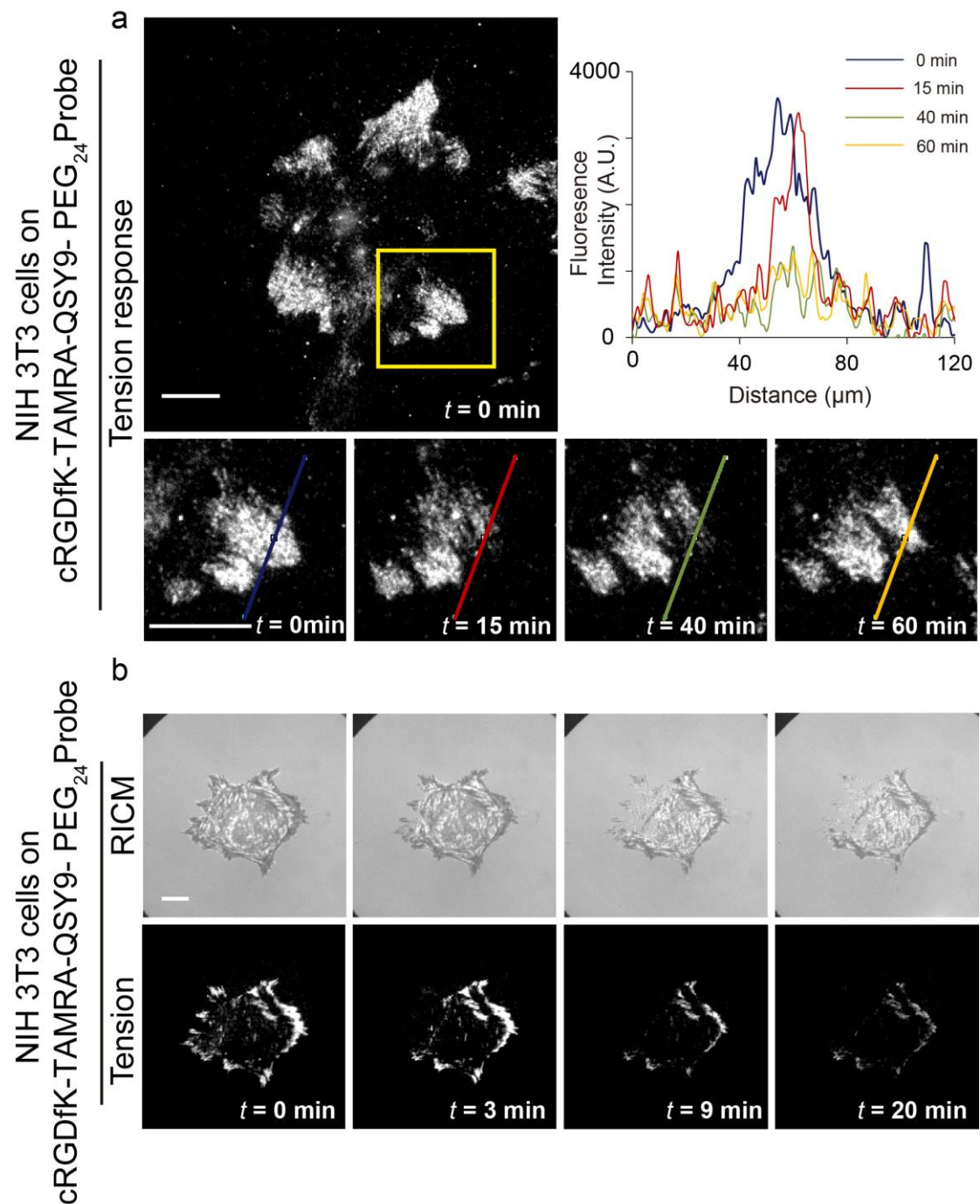
To co-localize the tension signal with β 3-integrin-GFP, rat embryonic fibroblast (REF) cells were transfected with GFP β 3-integrins and plated on the cRGDfK-TAMRA-QSY9/PEG₂₄ tension probe (**10a**) surface and imaged. At the 1 hr time point, the tension signal was highly co-localized with the GFP fluorescence, indicating that the β 3-integrins are primarily associated with the observed tension. Manders' Colocalization test was performed for 8 cells and the Manders' Colocalization Coefficients (MCC) was calculated to be 0.88 ± 0.08 (β 3-integrin-GFP over tension signal).⁵ (Scale bar 10 μ m)

Supplementary figure S11. Tension signal dissipates following PFA fixation



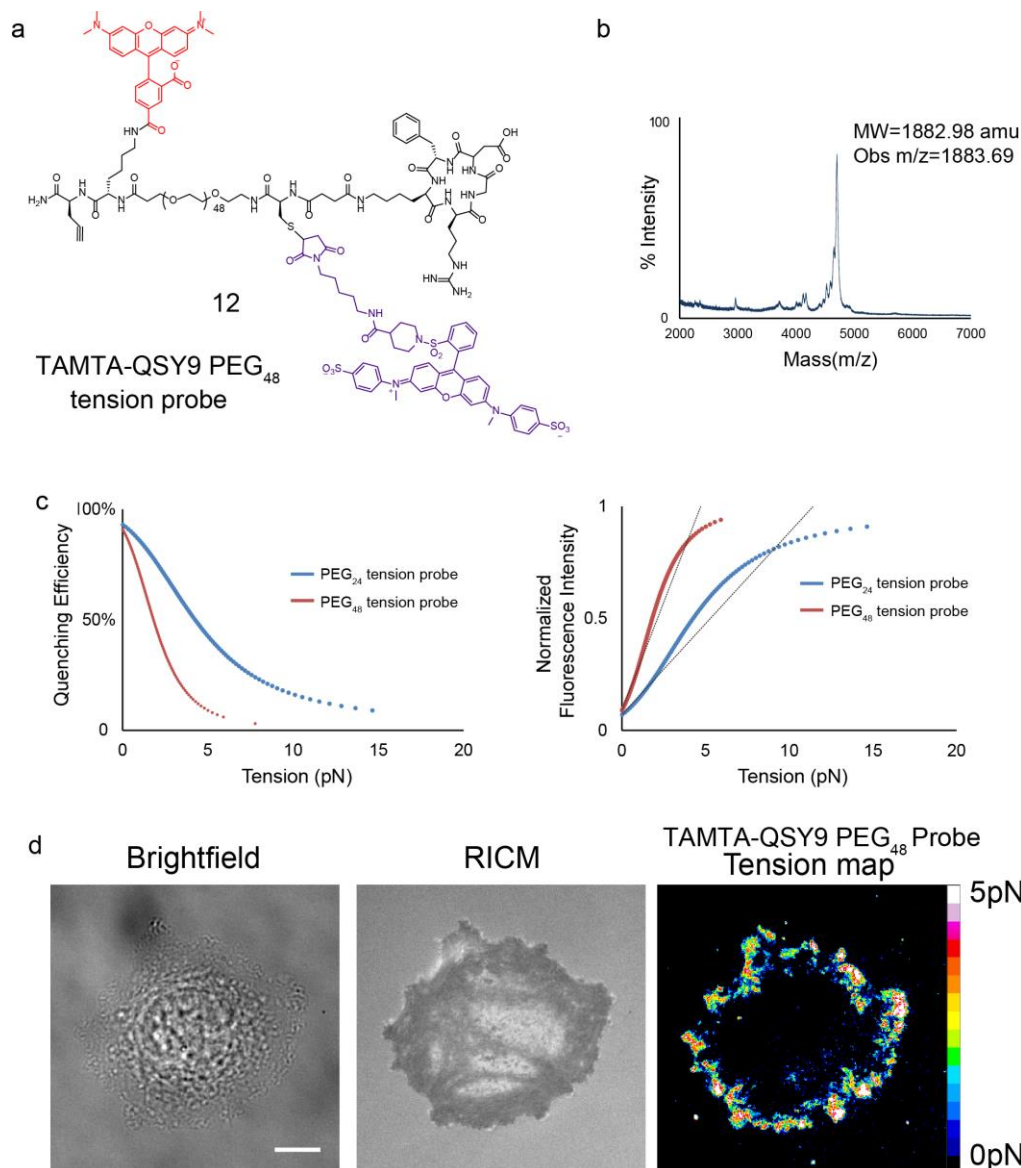
NIH 3T3 cells were plated onto the cRGDfK tension sensor (**10a**) surface for 1 hr and then imaged in RICM and tension signal channels. Representative images are shown to the right (Before fixation). Subsequently, cells were fixed by incubation in 1 ml of 4% w/v paraformaldehyde (PFA) for 10 min. The PFA was subsequently rinsed off using 25 ml of 1 X PBS, and then cells were permeated by incubation with 0.1% (v/v) Triton X-100 for 5 min in PBS. The cells were then rinsed with 25 ml 1 X PBS, and then blocked for 1 hr using 1% w/v BSA. The tension signal following fixation (left) was weakened and more diffuse, in agreement with literature. The PEG polymer is not crosslinked by PFA and because the cellular cytoskeleton likely relaxes following PFA treatment, the tension signal typically becomes weaker following PFA treatment.⁶ (Scale bar 10 μ m).

Supplementary figure S12. Tension signal is dynamic, reversible, and actin dependent



a) To analyze tension signal dynamics, 3T3 fibroblast cells were plated onto the cRGDfK tension sensor (10a) surface for 1 hr and then imaged using time lapse fluorescence microscopy. Line scan analysis confirms the dynamic nature of the tension signal. b) To verify that the tension response is reversible and actin dependent, 3T3 fibroblasts were treated with latrunculin B (latB) and then imaged. The signal rapidly diminished and returned to background levels within 20 min of treatment of latB. Scale bar = 10 μm .

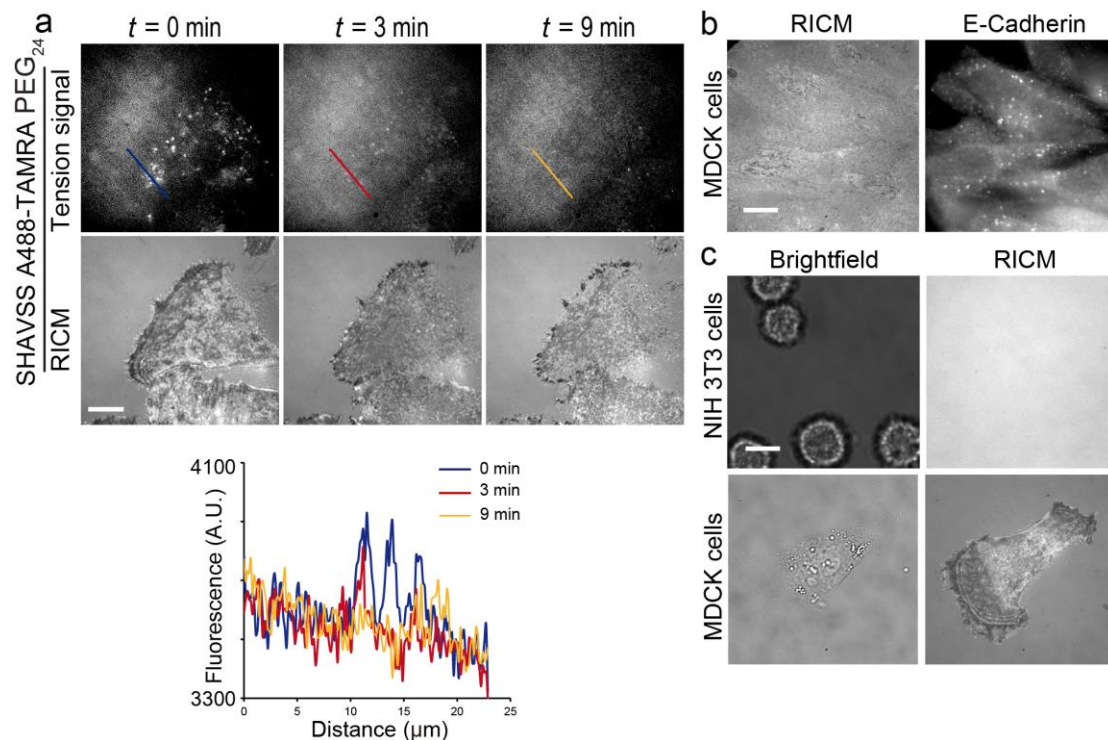
Supplementary figure S13. Dynamic range of PEG₄₈ and PEG₂₄ tension probes



a) The PEG₄₈-cRGDfK tension probe was manually synthesized using SPPS and coupled with cRGDfK ligand and quencher (QSY 9) following the protocols described in SI figure S1, figure S3 and figure S4. b) The synthesized construct (12) was purified by HPLC and its mass confirmed by MALDI-TOF MS. c) By using the WLC and Flory models, we generated a theoretical plot of quenching efficiency versus tension and fluorescence versus tension to compare PEG₂₄ and PEG₄₈ probes. The black lines in the fluorescence versus tension plot represent linear regression fits ($R^2=0.9$), which define the linear dynamic range of the PEG₂₄ tension probes (<15 pN) and PEG₄₈ tension probes (<5 pN). d) NIH 3T3 cells were plated onto the MTFM sensor modified glass surfaces for 1 hr to allow for cell adhesion. The images show representative brightfield, RCM, and tension map that indicate that PEG₄₈-based tension probes are active and perform similarly to the PEG₂₄-based probes despite the difference in dynamic range. This data supports the modularity of this approach in generating tension probes, allowing one to tune the dynamic range to appropriate levels that match the expected biophysical signaling system.

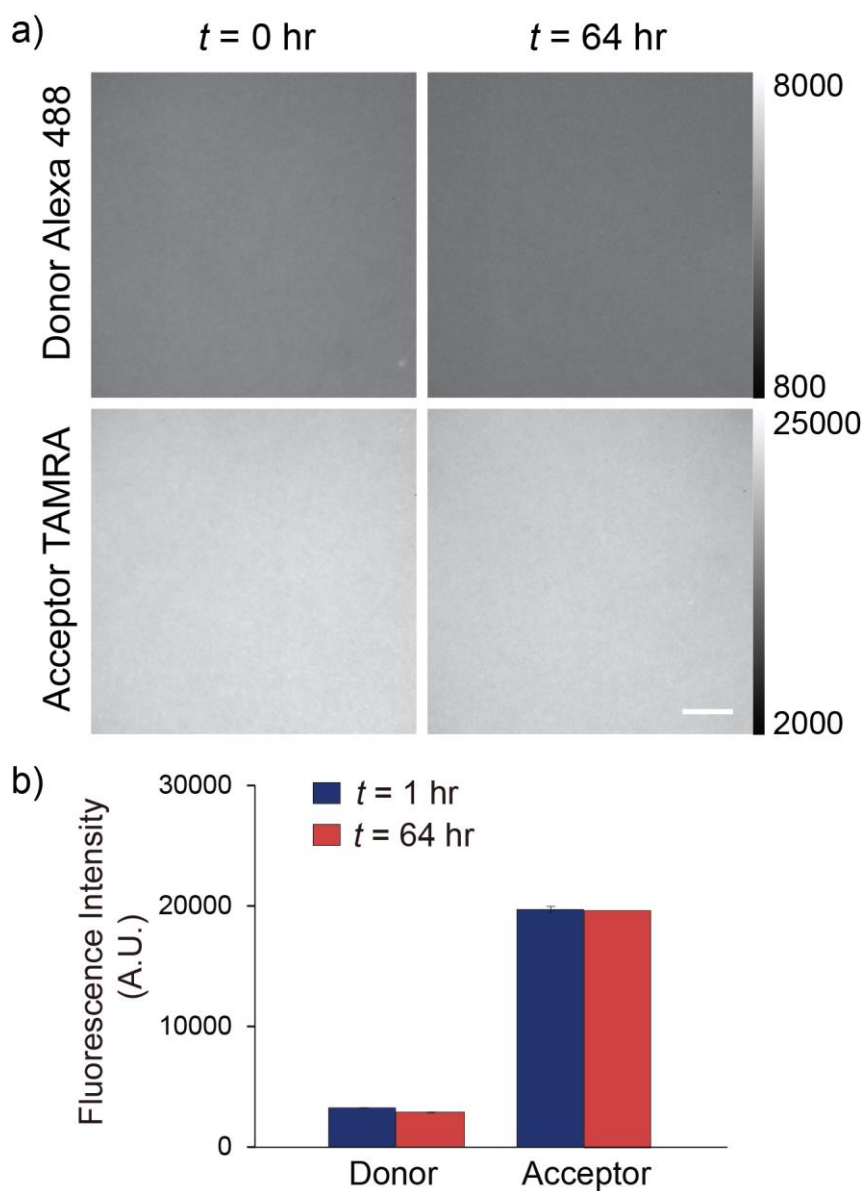
Scale bar = 10 μm.

Supplementary figure S14. SHAVSS tension response is actin dependent and likely E-cadherin specific



a) To validate that the E-cadherin signal is actin-dependent, MDCK cells were cultured onto SHAVSS probes modified surfaces for 6 hours, and then treated with 25 μM latB. After 9 min, the fluorescence signal completely dissipated and returned to background levels for all observed cells. b) To further validate that the tension signal is due to specific interaction of E-cadherin-SHAVSS ligand, MDCK cells were incubated on SHAVSS sensor modified surfaces for 6 hr and then fixed and immunostained for E-cadherin extracellular domain EC4. The results show the presence of E-cadherin puncta at the basal cell surface. These puncta resemble the signal observed for SHAVSS tension probe. Note that the tension signal significantly weakens once cells are fixed, likely due to nm scale cytoskeletal and PEG relaxation, and we are unable to obtain tension signals for fixed cells here. c) NIH3T3 fibroblasts were cultured onto SHAVSS sensor substrate, and minimal cell attachment was observed under same experimental conditions. This is in agreement with published E-cadherin expression levels for fibroblasts. Scale bar = 10 μm .

Supplementary figure S15. Fluorescence intensity change of MTFM probes over 64 hours



To test the stability of the MTFM probes, coverslips modified with TAMRA-Alexa488-PEG₂₄ probes were stored in cell culture media for 64 hours at 37 °C. Fluorescence intensity of donor (Alexa 488) and acceptor (TAMRA) was measured before and after incubation, and minimal change was observed (a and b). Note that by t=5 days, the donor and acceptor signal decreased, indicating degradation of the dyes. Data was obtained from 10 different regions in two different samples. Scale bar = 10 μ m.

Materials and Methods

(3-Aminopropyl) triethoxysilane (97%, APTES), triethylamine (99%, TEA), paraformaldehyde (95%, PFA), 1,3-Propanesultone (98%), N,N-Diisopropylethylamine (99.5%, DIEA), Hank's balanced salts (#H1387) and Triton X-100 were purchased from Sigma- Aldrich (St. Louis, MO) and used without further purification. All the Fmoc protected amino acids used in solid phase peptide synthesis and 5(6)-TAMRA, SE(# AS-81124-01), 5(6) - FAM, SE(#AS-81006) were purchased from Anaspec (Fremont, CA). The heterobifunctional linker azide-NHS (#88902) and azide-biotin (#10184) were purchased from Thermo Fisher Scientific (Rockford, IL). E-cadherin extracellular domain EC4 primary antibody was purchased from Santa Cruz Biotechnology (Dallas TX). The fluorescent dyes Alexa488-maleimide and Alexa647 labeled IgG1 secondary antibody were purchased from Life Technologies (Carlsbad, CA). Number two glass coverslips, ascorbic acid (>99.0%), and 96-well plates were purchased from Fisher Chemical & Scientific (Pittsburg, PA). DMF (>99.5%), DMSO (99.5%) and sodium bicarbonate (99.0%) were purchased from EMD chemicals (Philadelphia, PA)., mPEG-NHS (MW 2000) and mPEG-NHS (MW 5000) were purchased from Nanocs (New York, NY). Amine-PEG-SH (MW 3400) was purchased from Creative PEGworks (Winston Salem, NC). CuSO₄·5H₂O was purchased from Mallinckrodt (St. Louis, MO), and P4 gel size exclusion beads were acquired from BioRad (Hercules, CA). IgG1 paxillin-antibody was obtained from EMD Millipore (Billerica, MA). All DI water was obtained from a Nanopure water purification system with a UV sterilization unit and showed a resistivity of 18.2 MΩ.

Peptide synthesis.

Peptides ligands **2-5** were synthesized following the standard procedure using a Liberty CEM Microwave Automated Peptide Synthesizer (NC, USA) and a Fmoc-Rink Amide MBHA Resin (AnaSpec, CA, USA).

HPLC. All PEG conjugated products were purified by using a C18 column (diameter: 4.6 mm; length: 250 mm) in a reverse phase binary pump HPLC that was coupled to a diode array detector (Agilent 1100).

MALDI-TOF Mass spectroscopy. A 10 mM solution of 2,5-dihydroxybenzoic acid (DHB) was prepared in 1% TFA water: Acetonitrile 1:1 solution as the MALDI matrix. All products were also pre-dissolved in matrix solution. 2 µL of this mixture was added to each well on the MALDI plate. After allowing the solution to dry for 20 min, the sample was analyzed by a high performance MALDI time-of-flight mass spectrometer (Voyager STR).

Fluorescence microscopy. Living cells were imaged in standard cell imaging buffer (Hank's balanced salt, pH 7.4, 10 mM HEPES without phenol red) at 37 °C, and fixed cells were imaged in 1% BSA in 1x PBS at room temperature. During imaging, physiological temperature was maintained with a warming apparatus consisting of a sample warmer and an objective warmer (Warner Instruments 641674D and 640375). The microscope was Nikon Eclipse Ti driven by the Elements software package. The microscope features an Evolve electron multiplying charge-coupled device (EMCCD; Photometrics), an Intensilight epifluorescence source (Nikon), a CFI Apo 100x (numerical aperture (NA) 1.49) objective (Nikon). This microscope also includes the Nikon Perfect Focus System, an interferometry-based focus lock that allowed the capture of multipoint and time-lapse images without loss of focus. The microscope was equipped with the following Chroma filter cubes: FITC, TRITC, Cy5, and reflection interference contrast microscopy (RICM). The FITC, TRITC, Cy5 images were taken using 500 ms exposure time while RICM images were acquired using 10-20 ms exposure time. One additional cutoff filter (product number: 86354, Edmund optics, USA) was included into the optical path to eliminate the bleed-through from acceptor TAMRA into the FITC channel.

Cell culture. NIH 3T3 cells and rat embryonic fibroblast (REF) were cultured in DMEM medium (Mediatech) supplemented with 10% FBS (Mediatech), L-glutamine (2.1 mM, Mediatech), penicillin G

(100 IU ml⁻¹, Mediatech) and streptomycin (100 µg ml⁻¹, Mediatech) and were incubated at 37 °C with 5% CO₂. Cells were passaged at 90–100% confluency and plated at a density of 50% using standard cell culture procedures.

Preparation of small unilamellar vesicles phospholipids. (1,2-dioleoyl- sn-glycero-3- phosphocholine, DOPC; and 1,2-dioleoyl- sn-glycero-3-phosphoethanolamine-N-(cap biotiny), biotin-DPPE) were purchased from Avanti Polar Lipids (Alabaster, AL). To prepare small unilamellar vesicles, lipids were combined in a round bottom flask at the desired molar ratio in chloroform and dried on a rotary evaporator to form a lipid film. The film was dried under a stream of N₂ for 15 min and then resuspended with Nanopure water to achieve a lipid concentration of 2 mg/ml. The lipid solution was frozen in a dry ice-acetone bath and thawed in a 40°C water bath three times. The vesicles were passed through a 100 nm polycarbonate filter (Whatman, Florham Park, NJ) 10 times using a high-pressure extruder (Northern Lipids, Burnaby, Canada) warmed to 45°C.

Assembly of supported lipid membranes. To prepare the glass surface, a 96-well plate with #1.5 glass (Greiner Bio-One, Monroe, NC) was etched with 1 M NaOH for 1 hr and rinsed with Nanopure water. A 0.5 mg/ml vesicle solution prepared in phosphate buffered saline (PBS) (for biotin-DPPE) and added to the glass for 20 min to form the bilayer. The surfaces were blocked with 0.1 mg/ml bovine serum albumin for 30 min. The membranes were then incubated with 36 nM streptavidin (Rockland Immunochemicals, Gilberts- ville, PA) for 45 min. After rinsing unbound streptavidin, the surface was treated with 100 nM of biotinylated sample for 1 hr.

Supplementary Notes

1. Determination of the Förster distance of Alexa 488-TAMRA FRET pair and TAMRA-QSY9 FRET pair

To convert the fluorescence signal to the distance between the fluorophores, we used the FRET equation where quenching efficiency depends on the donor-to-acceptor/quencher separation distance r with an inverse 6th power law due to the dipole-dipole coupling mechanism. $QE = \frac{1}{1+(r/R_0)^6}$,⁷ in which R_0 is the Förster distance of this pair of donor and acceptor. To calculate the R_0 of the two donor and quencher/acceptor pairs (Alexa 488- TAMRA and TAMRA- QSY9), we measured the donor emission and acceptor/quencher absorption spectrum of these dyes. The R_0 was then calculated based on the overlap integral of the donor emission spectrum with the acceptor absorption spectrum and their mutual molecular orientation as expressed by

$$R_0^6 = \frac{9Q_0(\ln 10)\kappa^2 J}{128\pi^5 n^4 N_A}$$

⁷ where Q_0 is the fluorescence quantum yield of the donor in the absence of the acceptor, κ^2 is the dipole orientation factor, and $\kappa^2 = 2/3$ is assumed. n is the refractive index of the medium, N_A is Avogadro's number, and J is the spectral overlap integral calculated as

$$J = \int f_D(\lambda) \epsilon_A(\lambda) \lambda^4 d\lambda$$

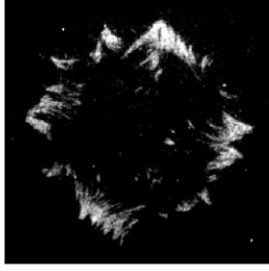
⁷ Fit to the FRET equation, Förster distance (R_0) is determined to be 6.4 nm, and 488 and TAMRA pair to be 5.9 nm.

2. Measuring the quenching efficiency (QE) of Alexa 488-TAMRA FRET pair and QSY9 and TAMRA-QSY9 FRET pair

The quenching efficiency of donor and quencher/acceptor is determined by the measurement of fluorescence intensity of the biotinylated donor only molecule and donor-quencher/acceptor molecule on supported lipid bilayer (SLB). The biotinylated molecules were synthesized by coupling a small molecule biotin-azide through click chemistry onto the alkyne group of the probes. Eight lipid bilayer surfaces were functionalized with streptavidin and then incubated with either donor only or donor-acceptor molecules of different concentration (50nM~400nM). The average fluorescence intensity for donor only surfaces was compared to the fluorescence intensity of surfaces containing both donor and acceptor in order to determine the quenching efficiency of the surfaces. The quenching efficiency is calculated to be $93.35\% \pm 0.05$ between TAMRA and QSY9 and $93.84\% \pm 0.04$ between Alexa 488 and TAMRA. All bilayer surfaces were tested for lateral mobility using FRAP experiments.

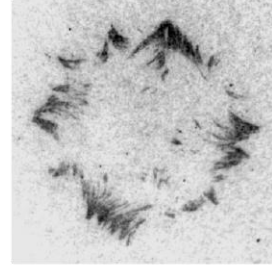
3. Stepwise image analysis of cell tension by using FRET and WLC models.

1). Effective fluorescence intensity (I_E)



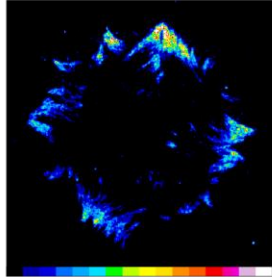
$$QE = 1 - \frac{I_E}{I_D}$$

2). Quenching efficiency image (QE)



$$z = R_0 * \left(\frac{1}{QE} - 1 \right)^{\frac{1}{6}} - z_0$$

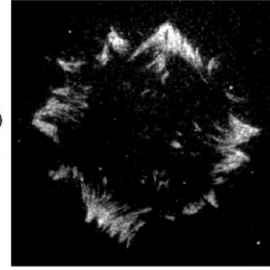
4). Tension map (F)



0 pN

20 pN

3). PEG extension image (z)



$$F = \frac{k_B T}{L_p} \left(\frac{z}{L_0} + \frac{1}{4 \left(1 - \frac{z}{L_0} \right)^2} - \frac{1}{4} + \sum_{i=2}^7 \alpha_i \left(\frac{z}{L_0} \right)^i \right)$$

I_E = Effective fluorescence intensity of the tension image, $I_E = I - I_B$ where I = fluorescence intensity of raw image, I_B = background produced by excess tension probes that cannot be used by limited numbers of integrins in unit area (300/um²).⁹

I_D = fluorescence intensity of donor only surface

R_0 = Förster radius, distance at which the energy transfer efficiency is 50%.

T = temperature (310 K)

L_p = persistence length (0.38 nm)

L_0 = contour length (24 x 0.35 = 8.40 nm for PEG₂₄ and 16.8 for PEG₄₈)

z_0 = distance between donor and acceptor at the resting state.

z = PEG extension

k_B = Boltzmann constant (1.38 x 10⁻²³ N*m/K)

The following image analysis steps were performed to estimate the magnitude of tension experienced by integrin receptors:

- 1) Collect raw fluorescence images of cells cultured on MTFM probes using indicated imaging parameters (see Optical Microscopy section in methods)
- 2) Subtract EMCCD instrumental background and acquire the raw tension image, I .
- 3) Determine the fluorescence intensity of the sensor at resting by averaging three regions of interest away from cells. Then divide this resting fluorescence intensity by (1- QE), thus yielding the

fluorescence intensity of fully de-quenched surface (I_D). Given that the probe density was measured to be 1060 ± 31 sensors/ μm^2 ,⁸ and beyond the maximum packing density of integrins of $300/\mu\text{m}^2$,⁹ we can estimate the background of non-accessible tension probes, which results in the background $I_B = I^*(1 - \frac{300}{1060})$. Based on this estimation, we can calculate the effective fluorescence intensity image ($I_E = I - I_B$.)

- 4) Subsequently, convert I_E image to QE image by applying the equation $QE = 1 - I_E/I_D$.
- 5) Apply the FRET equation $z = R_0 * (\frac{1}{QE} - 1)^{\frac{1}{6}} - z_0$ thus converting the quenching efficiency map (QE map) to the PEG extension, z .
- 6) Apply the extended WLC model $F = \frac{k_B T}{L_p} (\frac{z}{L_0} + \frac{1}{4(1 - \frac{z}{L_0})^2} - \frac{1}{4} + \sum_{i=2}^7 \alpha_i (\frac{z}{L_0})^i)$,¹⁰ to convert the z map into a tension map.

References:

- (1) Xiao, J.; Chen, R.; Pawlicki, M. A.; Tolbert, T. J. *J. Am. Chem. Soc.* **2009**, 131 (38), 13616.
- (2) Johnson, E. C. B.; Kent, S. B. H. *J. Am. Chem. Soc.* **2006**, 128 (20), 6640.
- (3) Estephan, Z. G.; Jaber, J. a; Schlenoff, J. B. *Langmuir* **2010**, 26 (22), 16884.
- (4) Galush, W. J.; Nye, J. a; Groves, J. T. *Biophys. J.* **2008**, 95 (5), 2512.
- (5) Dunn, K. W.; Kamocka, M. M.; McDonald, J. H. *Am. J. Physiol. Cell Physiol.* **2011**, 300 (4), C723.
- (6) Liu, Y.; Yehl, K.; Narui, Y.; Salaita, K. *J. Am. Chem. Soc.* **2013**, 135 (14), 5320.
- (7) *Introduction to Fluorescence Sensing*; Demchenko, A. P., Ed.; Springer Netherlands: Dordrecht, 2009.
- (8) Zhang, Y.; Ge, C.; Zhu, C.; Salaita, K. *Nat. Commun.* **2014**, 5, 5167.
- (9) Moore, S. W.; Roca-Cusachs, P.; Sheetz, M. P. *Dev. Cell* **2010**, 19 (2), 194.
- (10) Bouchiat, C.; Wang, M. D.; Allemand, J.; Strick, T.; Block, S. M.; Croquette, V. *Biophys. J.* **1999**, 76 (1), 409.